Improving thermoelectric properties of $Ca_3Co_4O_{9+\delta}$ through both Na doping and K addition at optimal values

Berdan Özkurt[1*], M. Ersin. Aytekin[2], M. A. Madre[3], A. Sotelo[3], M. A. Torres[3]

[1] Department of Energy Systems Engineering, Faculty of Technology, Tarsus University, 33400 Tarsus, Turkey

[2] Department of Nanotechnology and Advanced Materials, Graduate School of Natural and Applied Science, Mersin University, Mersin, Turkey

[3] Instituto de Ciencia de Materiales de Aragón (CSIC-Universidad de Zaragoza), Mª de Luna 3, 50018 Zaragoza, Spain.

Abstract

$Ca_{2.93}Na_{0.07}Co_4O_y$/x wt% K_2CO_3 (x=0.00, 0.01, and 0.03) polycrystalline ceramics were prepared by conventional solid-state method. XRD results have shown that all samples predominantly include $Ca_3Co_4O_9$ phase together with small amounts of secondary phases. SEM images show that all samples have randomly oriented plate-like grains in different sizes. The electrical resistivity measurement showed that electrical properties of $Ca_3Co_4O_9$ ceramics can be improved significantly by both, Na doping and K addition at their optimal values. The effect of dopants on thermoelectric properties of $Ca_3Co_4O_9$ was examined by both, Seebeck coefficient and power factor, being higher in K-added than in the pure samples, indicating that thermoelectric properties of samples are positively affected when alkaline elements enter into their structure.

Keywords: $Ca_3Co_4O_9$; XRD; SEM; Electrical resistivity; Seebeck coefficient; Power factor

* Corresponding author. Tel.: +90 324 627 4804; fax: +90 324 627 4805

E-mail address: berdanozkurt@tarsus.edu.tr

1. Introduction

Many harmful gases such as carbon dioxide and carbon monoxide are released to the atmosphere, by the extreme use of fossil fuels to produce energy, causing serious deteriorations in the Earth's ecosystems. It is obvious that wind and solar energy are reliable sources for clean energy production without the release of toxic gases. However, the energy must be used more efficiently to decrease global environmental risks, regardless of how it is produced. Therefore, thermoelectric (TE) materials, that have the capability of converting heat differences directly to electricity, can play a key role in applications for higher energy efficiency. On the other hand, the performance of TE materials can be evaluated by parameters such as Seebeck coefficient (S), electrical resistivity (ρ), phase stability, and thermal conductivity (κ). Most of these factors are included in the so-called Figure-of-Merit, ZT ($=S^2T/\rho\kappa$, T is absolute temperature). Consequently, it is very important to obtain TE materials with high S, and working temperatures, together with low ρ, and κ [1].

On the other hand, in spite of the relatively low TE performances of oxide materials, they can be improved by both doping using appropriate chemical elements such as Ag, Eu, Zr, or Ti [1-7] and fabrication methods in their preparation, such as hot pressing, spark plasma sintering, or laser floating zone [8-12]. It can be generally expected that the partial substitution of cations in electroceramic materials such as thermoelectrics and superconductors can provide useful changes in the carrier concentration, while optimizations in material preparation methods ensure higher grain orientation to provide the enhancement of electrical conductivity. Recently, the results of partial substitutions in ceramic superconductors using alkali metals, such as Li, Na,

and K, have been clearly shown that they lead to more homogeneous structures together with larger grain sizes owing to the formation of liquid phases [13-17]. Moreover, the eutectic composition of alkaline elements shows that their crystallization process begins at lower temperatures than those required for crystallization of ceramic materials [18-19]. Thus, when alkaline elements are doped into ceramic materials, nucleation and crystal growth can start at lower temperatures, leading to the formation of larger grains. Furthermore, co-doping works of alkaline elements in ceramic superconductors also showed that they had a significant effect on the size of grains [20-23]. Recently, Na doping in small amounts in $Ca_3Co_4O_9$ has shown that Na provides an important increase in mean grain sizes, decreasing electrical resistivity [24]. These results have encouraged us to further improve TE performances of $Ca_3Co_4O_9$ system through alkaline elements co-doping. The aim of this work is to study the effect of constant Na substitution for Ca ($Ca_{2.93}Na_{0.07}Co_4O_y$), with different wt.% K_2CO_3 additions (x=0, 1, 3, and 5), on the structural, microstructural, and thermoelectric properties of $Ca_3Co_4O_9$.

2. Experimental Procedure

$Ca_{2.93}Na_{0.07}Co_4O_y$/x wt% K_2CO_3 (x =0, 1, 3, and 5) polycrystalline samples were prepared through the conventional solid state reaction method from $CaCO_3$ (Panreac, 98+%), Na_2CO_3 (Panreac, 98+%), K_2CO_3 (Panreac, 98+%), and Co_3O_4 (Panreac, 98+%) powders. They were weighed in the appropriate proportions, mixed using an agate mortar and ball milled at 300 rpm for 30 minutes. After milling, the powders were subjected to a thermal treatment consisting in two different steps: 750 ^{0}C for 12 h and at 820 ^{0}C for 12 h, with an

intermediate milling in a ball mill for 2 hours at 300 rpm, in order to produce the total carbonates decomposition before the sintering process. The obtained homogeneous mixture was then pressed into 13 mm diameter pellets under 375 MPa applied pressure, followed by a sintering process at 900 ^{0}C for 24 h, under air, to produce the $Ca_3Co_4O_9$ phase.

Samples with x = 0, 1, 3, and 5 wt.% K_2CO_3 content will hereafter be named A, B, C, and D, respectively.

X-ray powder diffraction analyses were performed in a Rigaku Ultima IV X-Ray Diffractometer in the range 2θ = 3-60º to determine the phases present in the samples. Lattice parameters have been automatically calculated by the PDXL software version 1.6.0.1 with the ICDD version 6.0 database. The surface morphologies were performed on representative samples in a Zeiss/Supra 55 Scanning Electron Microscopy (SEM). Electrical resistivity and Seebeck coefficient were simultaneously determined by the standart dc four-probe technique in a LSR-3 measurement system (Linseis GmbH), in the steady state mode between 50 and 800 ^{o}C under He atmosphere. Moreover, with the electrical resistivity and thermopower data, the power factor has been calculated in order to determine the samples performances.

3. Results and discussion

Figure 1 shows the powder XRD patterns of $Ca_{2.93}Na_{0.07}Co_4O_y$/x wt% K_2CO_3 (x =0.0 ~ 0.03). The results indicate that all the samples mainly have $Ca_3Co_4O_9$ phase, with minor impurity phases. The intensity of diffraction peaks belonging to $Ca_3Co_4O_9$ phase at $\approx$8.22^o, 16.48^o, 24.84^o, and 33.4^o for all samples is quite high, indicating a good crystalline quality of the $Ca_3Co_4O_9$ phases. Moreover, any impurity phase based on element K in sample D was not

observed even if it has the highest amount of K, suggesting its incorporation in the unit cell of $Ca_3Co_4O_9$.

On the other hand, lattice parameters were determined from the XRD diffraction data, listed in Table 1, correspond to a monoclinic unit cell. These values are in accordance with the literature [25], and the differences between the samples can be due to the incorporation of dopants into $Ca_3Co_4O_9$ crystal structure. Moreover, from these graphs it seems evident that increasing the K addition, the main secondary phase $Ca_3Co_2O_6$ is transformed into $CaCo_2O_4$. Furthermore, grain thickness has been calculated by applying Scherrer equation on the peak appearing at 33.32 degrees. The results showed that it grows from around 35 nm for samples A, to around 55 nm for samples D. These results clearly indicate an important grain growth induced by potassium addition. This is due to the formation of a liquid phase (K_2CO_3) at the sintering temperature [26].

Figure 2 shows the SEM micrographs of all samples performed on fractured surfaces. They have similar grain morphology including the formation of plate-like grains even though they are randomly oriented. On the other hand, it is obvious that while high porosity is observed in sample A, K addition leads to its apparent reduction due to the higher cation diffusion rates induced by the liquid phase. Furthermore, grain sizes evaluated using image analysis software in several micrographs for each composition have shown that they are increased when K is added to the samples, reaching mean values of 1.64, 1.81, 1.88, and 1.89 μm for samples A, B, C, and D respectively. From these data, it can be deduced that K addition enhances, in an important manner, grain sizes, while the increase of K content only slightly raises them. This is due to the fact

that liquid phase increases cations mobility, compared with the typical processes without it.

Figure 3 presents ρ-T curves for all samples. It is worth mentioning that polycrystalline thermoelectric materials produced by solid state reaction are mainly composed of randomly oriented grains, as observed in Figure 2. The resistivity in all samples shows a significant decrease with increasing temperatures, exhibiting a semiconducting behaviour. ρ values for all K added samples are lower that the obtained in the undoped samples, in agreement with their lower porosity as observed in Figure 2. Sample C with 3 wt.% K_2CO_3 has the lowest resistivity values in the whole measured temperature range when compared with the other samples. The decrease of ρ depends also on hole carrier concentration and mobility [3,27,28], which can be increased in this case by doping and a rise in density. The minimum resistivity value at 800 ºC (15 mΩ cm) is lower than that measured in classically sintered materials (34-16.5 mΩ cm) and similar to those reported for materials prepared through advanced techniques (10–12.5 mΩ cm) [26,29-33]. From these data, it is clear that the process used in this work is useful to obtain low electrical resistivity materials, when compared with those composed of randomly oriented grains, which is favourable for increasing power factor [34,35]. Therefore, it is also important to improve the electrical properties of $Ca_3Co_4O_9$ ceramics to enhance their thermoelectric performance.

As it is well known, the temperature dependence of electrical conductivity, in the semiconducting zone, is described through the following equation:

$$\sigma.T \propto \exp(-E/k_B.T)$$

where E, k_B, and T are the activation energy, Boltzmann constant, and absolute temperature, respectively. The activation energy values can be obtained as the curve fit slope in the log (σT) *versus* 1/T plot below T*, as shown in Figure 4, where log (σT) *versus* 1000/T is represented. T* is the temperature where the behaviour of the samples changes from semiconducting to metallic. The values are around 44, 42, 40, and 46 meV, for samples A, B, C, and, D, respectively. These data confirm that K additions do not significantly modify the $Ca_3Co_4O_9$ conduction band, in agreement with previous works [30]. On the other hand, in the figure it can be seen that the data are higher when K_2CO_3 is added up to 3 wt.%, slightly decreasing for further additions. Under the assumption that these changes are mainly due to variations on the holes concentration, the estimated carrier concentration is increased when K is added to the samples. This fact can be explained by a partial substitution of Ca^{2+} in the structure by K^+ cations, which decreases the oxidation state of the Rock Salt layer, resulting in a higher amount of Co^{4+} in the conducting layer and increasing the charge carrier concentration.

Figure 5 shows the variation of the Seebeck coefficient with temperature for all samples. S values are positive in the whole measured temperature range, indicating that holes are responsible for the conduction mechanism. The Seebeck coefficient of all samples raises when the temperatures are increased. This similar behavior can be expected, since the $Ca_3Co_4O_9$ phase is the major one in all samples, as seen from XRD. Sample C displayed the highest S values at temperatures between 50 and 550^{o}C. Even if all S values overlap within the temperature range of 550-700^{o}C, sample C maintains its highest S values at 800^{o}C. This maximum value at 800 ºC (200 μV/K) is in the order of the

reported for materials sintered classically, or prepared through alternative methods (155-230 μV/K) [26,29-33].

The thermoelectric performance of samples, evaluated through their power factor ($PF=S^2/\rho$) as a function of temperature, is presented in Figure 6. In the graph it can be observed that PF increased with temperature in all cases. Moreover, K_2CO_3 addition significantly increases PF until 3 wt.%, slightly reducing it for higher K content. The highest PF at 800ºC has been determined in 3 wt.% K_2CO_3 samples (0.28 mW/K^2m), which is in the order of those reported for materials sintered classically, or prepared through alternative methods (0.14-0.42 mW/K^2m) [26,29-33].

4. Conclusions

In summary, $Ca_{2.93}Na_{0.07}Co_4O_y$/x wt.% K_2CO_3 (x =0, 1, 3, and 5) thermoelectric ceramics have been successfully fabricated by solid-state reaction method. It was found that all K-added samples possess lower ρ values than the undoped ones. Moreover, S values are maximized for 3 wt.% K_2CO_3 addition, leading to high PF values. These measurements clearly indicate that the addition of alkaline elements in appropriate proportions into $Ca_3Co_4O_9$ ceramic provides the enhancement of its thermoelectric properties.

Acknowledgements

All samples have been prepared in the Material Preparation Laboratory in Tarsus University in Turkey. As XRD and SEM measurements have been made in the MEİTAM Central Laboratory in Mersin University, other measurements in this study have been made in the Laboratory of Instituto de Ciencia de

Materiales de Aragón (CSIC-Universidad de Zaragoza). B. Özkurt and M.E Aytekin are supported by the BAP Research Fund of Mersin University, Mersin, Turkey, under Grand Contracts No:2018-3-TP3-3086. M. A. Madre, M. A. Torres, and A. Sotelo acknowledge the Spanish MINECO-FEDER (MAT2017-82183-C3-1-R), and the Gobierno de Aragón-FEDER (Research Group T 54-17R) for funding.

References

[1] Y. Wang, Y. Sui, J. Cheng, X. Wang, W. Su, J. Alloys Compd. 477, 817 (2009)

[2] Y. Lin, S. Sun, Q. Zhang, H. Shen, Q. Shao, L. Wang, W. Jiang, W. Jiang, Mater. Today Commun. 6, 44 (2016)

[3] A. Bhaskar, Y. C. Huang, C.-J. Liu, Solid State Comm. 168, 24 (2013)

[4] A. Sotelo, Sh. Rasekh, M. A. Torres, M. A. Madre, J. C. Diez, Adv. Appl. Ceram. 116, 383 (2017)

[5] R. K. Gupta, R. Sharma, A. K. Mahapatro, R. P. Tandon, Physica B 483, 48 (2016)

[6] L. Xu, F. Li, Y. Wang, J. Alloys Compd. 501, 115 (2010)

[7] F. Kahraman, M. A. Madre, Sh. Rasekh, C. Salvador, P. Bosque, M. A. Torres, J. C. Diez, A. Sotelo, J. Eur. Ceram Soc. 35, 3835 (2015)

[8] D. Kenfaui, D. Chateigner, M. Gomina, J. G. Noudem, Int. J. Appl. Ceram. Technol. 8, 214 (2011)

[9] J. G. Noudem, D. Kenfaui, D. Chateigner, M. Gomina, Scr. Mater. 66, 258 (2012)

[10] N. Y. Wu, T. C. Holgate, N.V. Nong, N. Pryds, S. Linderoth, J. Eur. Ceram. Soc. 34, 925 (2014)

[11] J. C. Diez, Sh. Rasekh, M. A. Madre, E. Guilmeau, S. Marinel, A. Sotelo, J. Electron. Mater. 39, 1601 (2010)

[12] N. M. Ferreira, Sh. Rasekh, F. M. Costa, M. A. Madre, A. Sotelo, J. C. Diez, M. A. Torres, Mater. Lett. 83, 144 (2012)

[13] B. Özkurt, J. Mater. Sci. Mater. Electron. 24, 2426 (2013)

[14] B. Özkurt, J. Supercond. Nov. Magn. 27, 2407 (2014)

[15] B. Özkurt, J. Supercond. Nov. Magn. 28, 1501 (2015)

[16] O. Bilgili, Y. Selamet, K. Kocabaş, J. Supercond. Nov. Magn. 21, 439 (2008)

[17] B. Özçelik, M. Gürsul, A. Sotelo, M. A. Madre, J. Mater. Sci. Mater. Electron. 26, 2830 (2015)

[18] Khalid Al-Ali, Satoshi Kodama, Hiroshi Kaneko, Hidetoshi Sekiguchi, Yutaka Tamaura, M. Chiesa, SolarPACES 2012, Sep 2012, Marrakech, Morocco. https://hal.archives-ouvertes.fr/hal-00870837

[19] A. D. Pelton, C. W. Bale, P. L. Lin, Calculation of phase diagrams and thermodynamic properties of 14 additive and reciprocal ternary systems containing Li_2CO_3, Na_2CO_3, K_2CO_3, Li_2SO_4, Na_2SO_4, K_2SO_4, LiOH, NaOH, and KOH, Can. J. Chem. 74 402 (1996)

[20] B. Özkurt, J. Mater. Sci. Mater. Electron. 25, 3295 (2014)

[21] M. Çalış, B. Özkurt, M. E. Aytekin, E. Gün, M. E. Kır, U. Öztornacı, J. Mater. Sci. Mater. Electron. 27, 2670 (2016)

[22] M. E. Kır, B. Özkurt, M. E. Aytekin, Physica B 490, 79 (2016)

[23] B. Özkurt, J. Mater. Sci. Mater. Electron. 28, 8857 (2017)

[24] G. Constantinescu, Sh. Rasekh, M. A. Torres, P. Bosque, J. C. Diez, M. A. Madre, A. Sotelo, Ceram. Int. 41, 10897 (2015)

[25] C. Zhu, Z. Li, H. An, G. Tang, D. Hou, J. Electron. Mater. 43, 3666 (2014)

[26] A. Sotelo, F. M. Costa, N. M. Ferreira, A. Kovalevsky, M. C. Ferro, V. S. Amaral, J. S. Amaral, Sh. Rasekh, M. A. Torres, M. A. Madre, J. C. Diez, J. Eur. Ceram. Soc. 36, 1025 (2016)

[27] A. C Masset, C. Michel, A. Maignan, M. Hervieu, O. Toulemonde, F. Studer, B. Raveau, J. Hejtmanek, Phys. Rev. B 62, 166 (2000)

[28] D. Wang, L. Cheng, Q. Yao, J. Li, Solid State Comm. 129, 615 (2004)

[29] J. G. Noudem, D. Kenfaui, D. Chateigner, M. Gomina, J. Electron. Mater. 40, 1100 (2011)

[30] G. Constantinescu, S. Rasekh, M. A. Torres, J. C. Diez, M. A. Madre, A. Sotelo, J. Alloys Compd. 577, 511 (2013)

[31] Sh. Rasekh, M. A. Torres, G. Constantinescu, M. A. Madre, J. C. Diez, A. Sotelo, J. Mater. Sci. Mater. Electron. 24, 2309 (2013)

[32] T. Schulz, J. Töpfer, J. Alloys Compd. 659, 122 (2016)

[33] Y. N. Li, P. Wu, S. P. Zhang, S. Chen, D. Yan, J. G. Yang, L. Wang, X. L. Huai, Chin. Phys. B 27, 057201 (2018)

[34] M. Ito, D. Furumoto, Scripta Mater. 55, 533 (2006)

[35] M. Mikami, N. Ando, R. Funahashi, J. Solid State Chem. 178, 2186 (2005)

Table 1. Lattice parameters

Samples	a(Å)	b(Å)	c(Å)
A	4.832	4.572	10.836
B	4.832	4.572	10.836
C	4.838	4.578	10.848
D	4.838	4.578	10.848

Figure captions

Fig. 1 Powder XRD patterns of samples A, B, C, and D.

Fig. 2. SEM micrographs obtained on fractured surfaces of (a) A, (b) B, (c) C and (d) D samples

Fig. 3. Resistivity as a function of temperature curves as a function of K content in $Ca_{2.93}Na_{0.07}Co_4O_y$/x wt.% K_2CO_3 (x =0, 1, 3, and 5) samples.

Fig. 4. Log (σT) *vs* 1000/T plot for all $Ca_{2.93}Na_{0.07}Co_4O_y$/x wt.% K_2CO_3 (x =0, 1, 3, and 5) samples. T* indicates the metallic-to-semiconducting transition temperature. The drawn lines are guides for the eyes.

Fig. 5. Temperature dependence of Seebeck coefficient as a function of K content in $Ca_{2.93}Na_{0.07}Co_4O_y$/x wt.% K_2CO_3 (x =0, 1, 3, and 5) samples.

Fig. 6. Temperature dependence of the power factor as a function of K content in $Ca_{2.93}Na_{0.07}Co_4O_y$/x wt.% K_2CO_3 (x =0, 1, 3, and 5) samples.

Figure 1

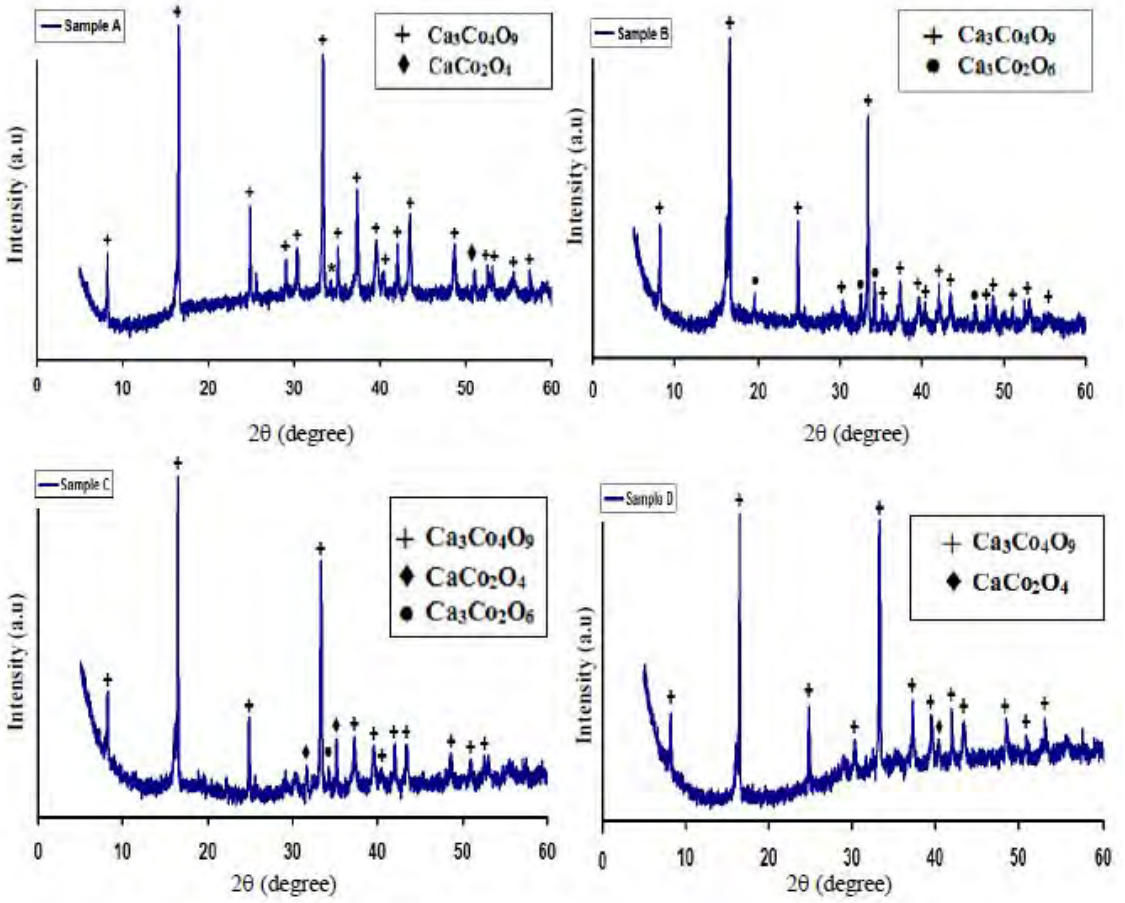
Sample A
+ Ca3Co4O9
♦ CaCo2O4
Intensity (a.u)
2θ (degree)
Sample B
+ Ca3Co4O9
● Ca3Co2O6
Intensity (a.u)
2θ (degree)
Sample C
+ Ca3Co4O9
♦ CaCo2O4
● Ca3Co2O6
Intensity (a.u)
2θ (degree)
Sample D
+ Ca3Co4O9
♦ CaCo2O4
Intensity (a.u)
2θ (degree)

Figure 2

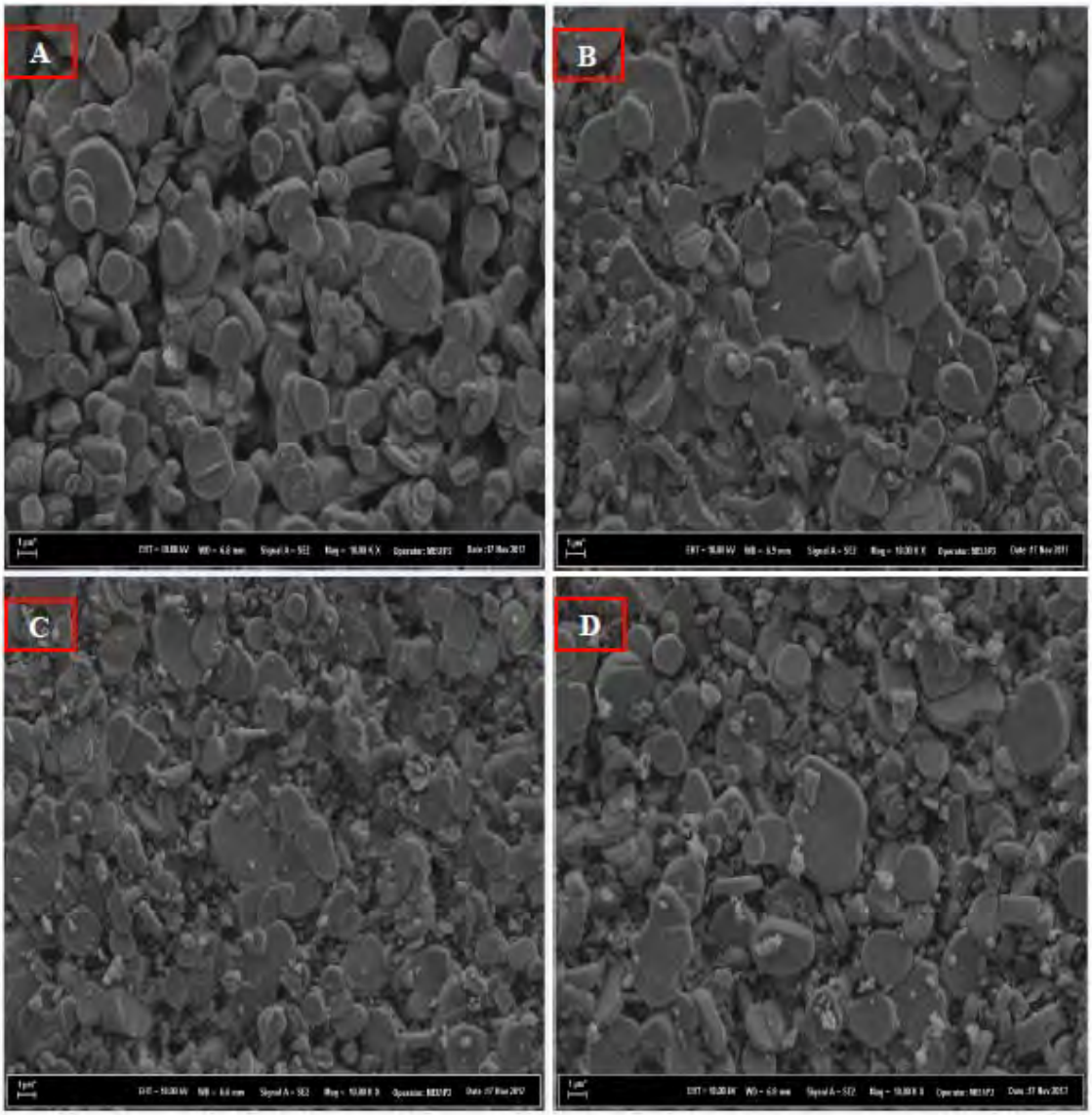

Figure 3

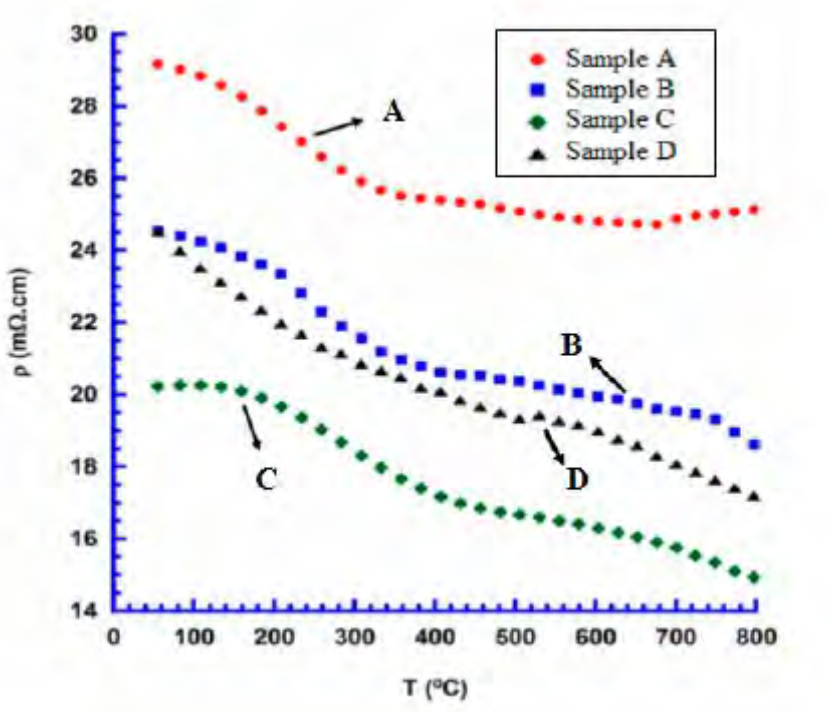
Sample A
Sample B
Sample C
Sample D
A
B
C
D
ρ (mΩ.cm)
T (°C)
30
28
26
24
22
20
18
16
14
0
100
200
300
400
500
600
700
800

Figure 4

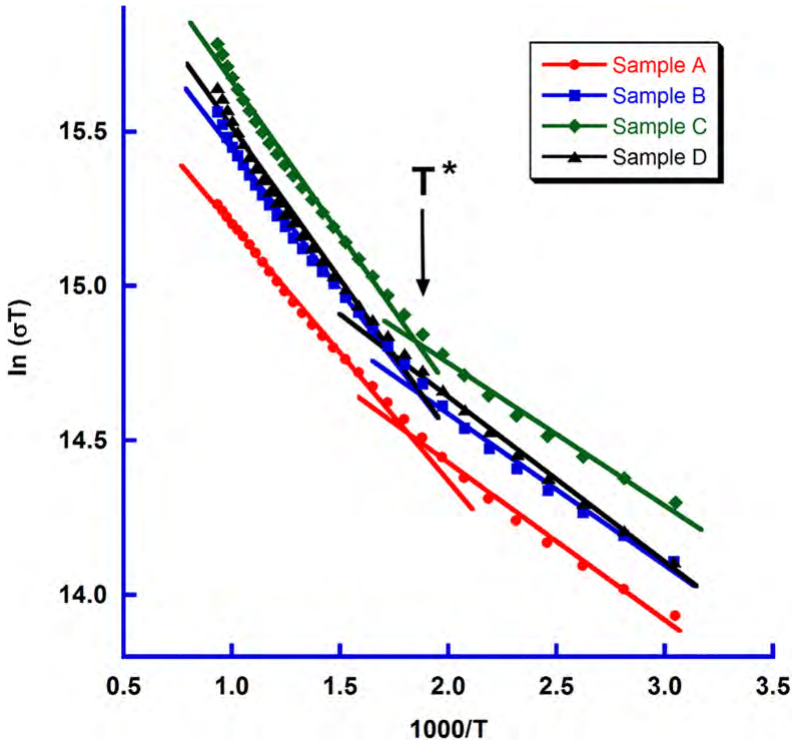
Sample A
Sample B
Sample C
Sample D
T*
15.5
15.0
14.5
14.0
ln (σT)
0.5
1.0
1.5
2.0
2.5
3.0
3.5
1000/T

Figure 5

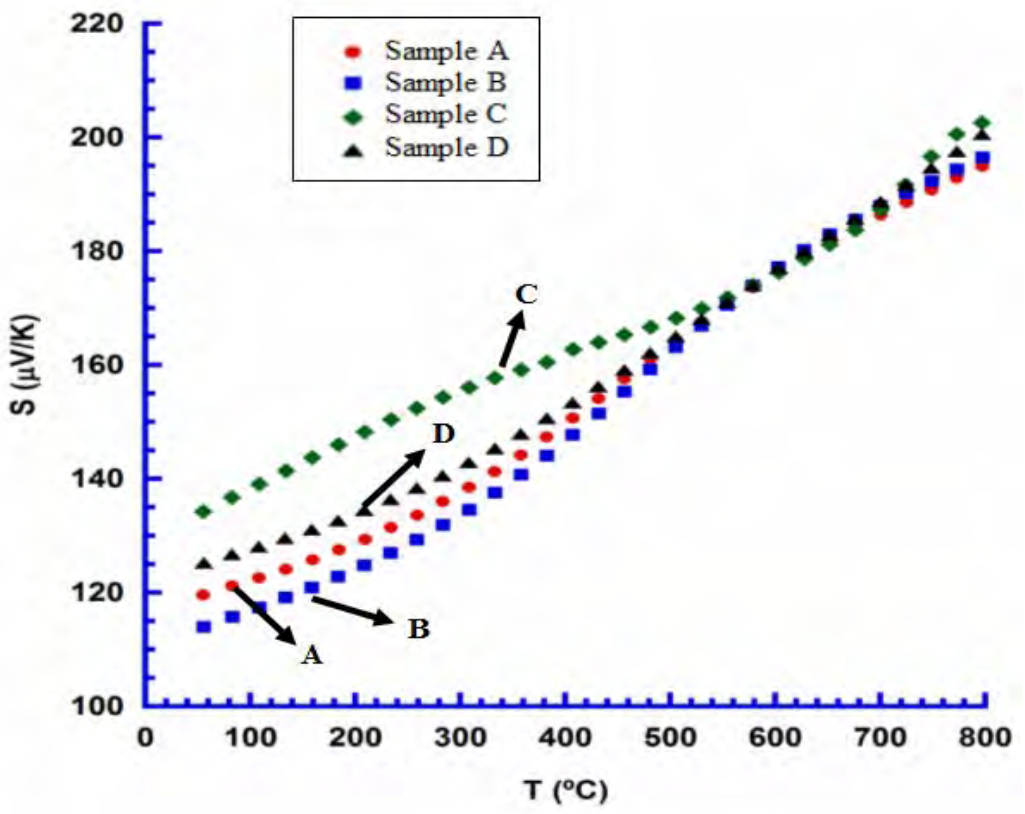
Sample A
Sample B
Sample C
Sample D
A
B
C
D
S (μV/K)
T (°C)
220
200
180
160
140
120
100
0
100
200
300
400
500
600
700
800

Figure 6

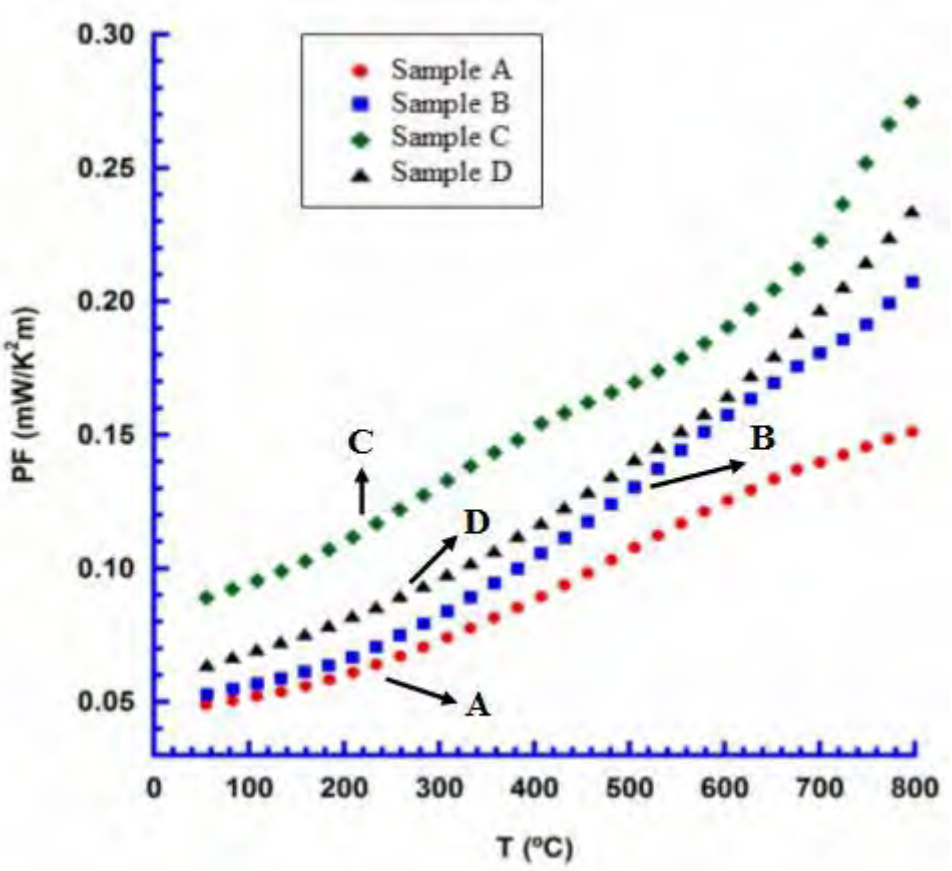
Sample A
Sample B
Sample C
Sample D
PF (mW/K²m)
T (°C)
0.30
0.25
0.20
0.15
0.10
0.05
0
100
200
300
400
500
600
700
800
A
B
C
D